IEEE Access
Multidisciplinary ⋮ Rapid Review ⋮ Open Access Journal

Received March 26, 2021, accepted April 12, 2021, date of publication April 16, 2021, date of current version May 18, 2021.

Digital Object Identifier 10.1109/ACCESS.2021.3073681

Multi-Points Indoor Air Quality Monitoring Based on Internet of Things

ZHIBIN LIU[1], GUANGWEN WANG[2], LIANG ZHAO[2,3], AND GUANGFEI YANG[4,5]

[1]College of Civil Engineering, Dalian Minzu University, Dalian 116600, China
[2]School of Control Science and Engineering, Dalian University of Technology, Dalian 116024, China
[3]Key Laboratory of Intelligent Control and Optimization for Industrial Equipment of Ministry of Education, Dalian University of Technology, Dalian 116024, China
[4]Institute of Systems Engineering, Dalian University of Technology (DUT), Dalian 116024, China
[5]DUT Artificial Intelligence Institute, Dalian 116023, China

Corresponding author: Liang Zhao (zliang@dlut.edu.cn)

This work was supported in part by the National Natural Science Foundation of China under Grant 61803067, Grant 71671024, and Grant 42071273; in part by the NSFC Guidance Program Projects of Liaoning Province under Grant 2019-ZD-0174; and in part by the Fundamental Research Funds for the Central Universities of China under Grant DUT20JC45 and Grant DUT20JC15.

ABSTRACT Indoor air quality monitoring is of great importance to human health as people typically spend more than 90% of their time in indoor environments. An indoor air quality detector (IAQD) enabling measurement of CO_2, PM2.5, temperature, humidity, has been designed and tested in residential buildings based on Internet of Things (IoT). The hardware and software design of IAQD are described in detail, and seven IAQDs with Zigbee wireless module embedded were deployed in the target building for a continuous period of one month in winter. The gateway collects sensor data from each IAQD in turn at an interval of two minutes, and transmits data to server in the cloud via GPRS/4G. The authorized users can access cloud platform via mobile apps or the Web browser. Monitoring data analysis results reveal that the maximum PM2.5 concentrations is 10 times than usual during cooking period, and CO_2 concentrations with the door closed will rise to 2500 ppm compared to the door opened at night, which threatens the health of occupants.

INDEX TERMS Indoor air quality, Internet of Things, sensors, Zigbee.

I. INTRODUCTION

Statistical studies showed that people spend more than 90% of their time in indoor environment [1], [2], and indoor air quality (IAQ) is one of the most important factors affecting human health. Temporary or long-term staying indoor exposure with poor air quality can lead to rapid or chronic illness. The short term effects include headache, dizziness, fatigue, as well as eyes and throat irritation, and chronic diseases include respiratory diseases, heart disease and cancer [3]. For example, long-term exposure to VOCs can cause damage to the liver, kidneys, and central nervous system [4], and high concentration of carbon dioxide (CO_2) will cause a higher respiratory rate, increased heart rate, or headache [5]. PM2.5 is considered the most harmful particulate matter to human health out of all atmospheric particulate matters. PM2.5 pollution is related to 220,000 lung cancer deaths worldwide each year, according to atmospheric models [6].

Due to previous researches, real-time indoor air quality monitoring is essential, and knowing the quality of air in house is important for assessing the involved risks. Traditionally, indoor air quality testing in the living environment is a service provided by professional environmental testing agency. The instruments used by organization are also expensive, and real-time data measurement is not available. On the other hand, because of the high price, not everyone can afford them. At present, with the development of Internet of Things (IoT), sensor, and electronic technologies, lots of portable real-time air quality monitoring detectors are proposed [4], [7]–[13].

In this paper, we design and implement an integrated indoor air quality detector (IAQD) based on IoT technology. A prototype of IAQD is proposed based on STM32 microcontroller, integrated PM2.5, CO_2, temperature and humidity sensors. The contribution of this paper is as follows:

The associate editor coordinating the review of this manuscript and approving it for publication was Yassine Maleh.

- A multi-point monitoring system is implemented for the indoor environment, and six rooms in the residence are monitored in real time, including living room, bedrooms, kitchen and bathroom. In addition, outdoor environmental parameters are also measured for comparative analysis.
- The influence of the external environment on the indoor air is studied by opening and closing doors and windows in winter.
- A month-long monitoring is conducted to study the relationship between the changes of air parameters and human behavior patterns and activity trajectories.

The rest of the paper is structured as follows. Section II presents the related works about indoor air quality monitoring in recent years. Section III details hardware and software architecture of proposed IAQD. The description of sensors and wireless network are also given here. Section IV presents the application of multi-points monitoring system and data analysis results. Finally, the conclusion of this paper is given in Section V.

II. RELATED WORK

There are lots of previous researches being proposed and making significant contributions in the area of indoor air monitoring, which will be discussed in the present section. The types of buildings monitored include residential buildings, museums, campus, hospitals, offices. A summary of related researches on the indoor air quality monitoring during the past decade is shown in Table 1.

Some studies focus on one certain indoor air parameter. Spachos and Hatzinakos [14] and Marques *et al.* [15] paid attention to monitoring CO_2 concentrations in offices and laboratories, respectively. Firdhous *et al.* [16] proposed an IoT-based indoor air quality monitoring system, which is limited to monitor O_3 concentrations in the office. In [17], the researchers monitored PM2.5 concentration in universities in northern China for up to 1 year. The indoor and outdoor concentrations of PM2.5 were analyzed in different seasons. More studies researched on the effects of a variety of indoor air parameters. Benammar *et al.* [18] presented a modular indoor air quality monitoring system based on IoT, and collected several types of sensor data such as CO_2, CO, SO_2, NO_2, O_3, temperature, and humidity. In addition, the performance of system was tested in Qatar University campus. The evaluation results for network showed that packet loss is serious in the cases of double or triple concrete wall obstacles. In [19], authors monitored the office's indoor air quality, including CO_2, O_2, VOC, for four consecutive days in summer. Chamseddine *et al.* [20] described a monitoring system in a hospital environment using several air quality indicators, including CO, CO_2, PM2.5, PM10 and TVOC. The results call for the adoption of remedial control measures to improve the indoor air quality in hospitals.

For residential buildings, Nica [21] implemented a real-time monitoring system to collect the indoor temperature, humidity and CO_2 concentration in a small two-story house. In [22], authors monitored the concentrations of CO, CO_2, PM10, PM2.5 and VOCs in eight typical SDUs for 48 hours in Hong Kong, China. SDUs are mainly for low-income families, with a typical floor area of merely 9.3 m^2. Monitoring results showed that, during open cooking, the maximum concentrations of PM2.5 reached up to 500 $\mu g/m^3$, which poses a threat to the health of occupants. Svertoka *et al.* [23] combined the three environmental parameters of PM2.5, PM10, and NO_2 perceived by the sensor, and proposed a decision support algorithm. Through a graphical interface, ordinary users can observe the measurement results in the client, receive danger warnings and decision support suggestions. Burghele *et al.* [24] used solid state nuclear track detectors to passively monitor radon and CO_2 footprint in ten houses, and proposed personalized mitigation measures to meet residents' health and comfort needs.

The indoor air quality monitoring detectors used in related works can be divided into two categories. One is commercial instruments, most of which are expensive. In most of these studies, the data collected by commercial instruments are stored in SD card, and regularly exported to the computer for analysis by manual. Another is the IoT-based remote monitoring system, the advantage of which is that users can access data at any time via web browser, supporting online visual chart, and the data can be exported online. The latter method will be more popular of indoor air quality monitoring in the future. The method adopted in this paper is online monitoring, which is more convenient than the local display architecture in some of the above related studies.

For the scale of monitoring points, researchers mostly focus on measuring the environmental quality of a room in multiple buildings. It has been proved to have important research significance for multi-point measurement in a building, such as the monitoring scenes of offices with different numbers of people, the monitoring of meeting rooms and offices with different room properties, and the environmental quality measurement of rooms with different functions in the hospital [14], [20]. In the residential monitoring, there is little research on multi-point monitoring in a building, especially in modern family rooms with different functions. In this paper, the developed environmental monitoring instrument is applied to the residential monitoring, and the relationship between the property of the room in the family and the environmental parameters is considered.

III. SYSTEM DESIGN AND IMPLEMENTATION

A. GENERAL DESCRIPTION

The diagram of the IAQ monitoring system based on IoT is shown in Fig. 1. All IAQDs are connected via a Zigbee wireless sensor network. The collector gateway sends acquisition instructions through the coordinator in the format of Modbus RTU (remote terminal unit), and each IAQD can be connected to the network as an End-device or Router-node. Collector gateway transmits all the data to the database in the cloud, and

TABLE 1. A summary of related literatures on real-time IAQ monitoring.

Ref.	Year	Building Types	Monitoring period	IAQD	Parameters*	Network	Archi*	No. monitoring points in a building	Room type
[14]	2016	Office	30 days in spring	Developed	C_2	Radio	Local display	5	Multiple
[16]	2017	Office	1 day in summer	Developed	O_3	Bluetooth	Local display	1	Single
[21]	2018	Residential	4 days in spring	NA	T, H, C_2	None	Local display	1	Single
[18]	2018	Library in campus	30 day in winter	Developed	T,H,C,C_2,O_3,N,S	Zigbee	IoT platform	1	Single
[19]	2018	Office	4 days in summer	Developed	T,H,O_2,C_2,V	VLC	IoT platform	2	Multiple
[15]	2019	Laboratory	1 day	Developed	C_2	WiFi	IoT platform	1	Single
[20]	2019	Hospital	1 hour in each season	Commercial	C, C_2, P, V	None	Local display	12	Multiple
[22]	2019	Residential	2 days in summer	Commercial	C, C_2, P, V	None	NA	1	Single
[17]	2020	Campus	1 hour in each season	Commercial	P	None	NA	1	Single
[23]	2020	Campus	None	Commercial	P, N	None	IoT platform	1	Single
[24]	2021	Residential	More than 1 year	Commercial	Radon, C_2	None	NA	1	Single
Ours	2021	Residential	30 days in winter	Developed	T,H,P,C_2	Zigbee	IoT platform	7	Multiple

*P-particulate matter (PM2.5, PM10), N-nitrogen dioxide, S-sulfur dioxide, C-carbon monoxide, C_2-carbon dioxide, O_3-ozone, T-temperature, H-humidity, V-volatile organic compounds, VLC- visible light communication, Archi-architecture.

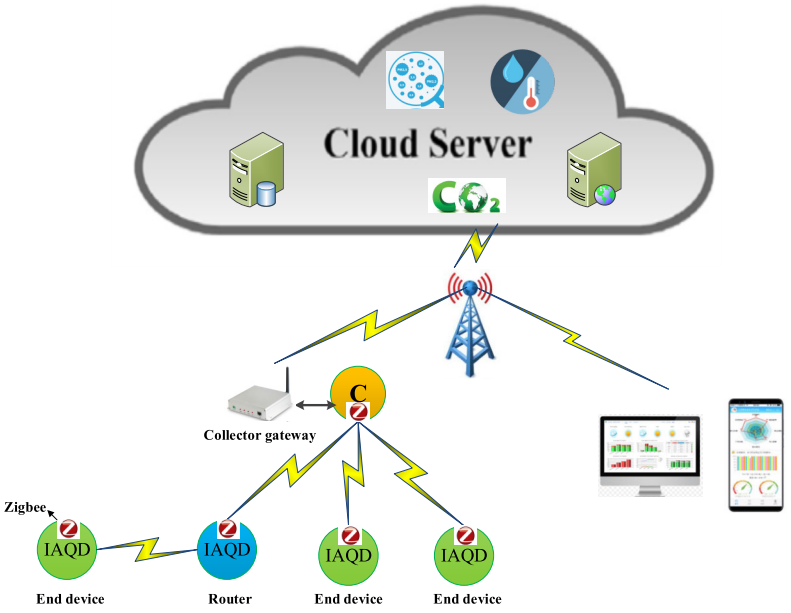

FIGURE 1. System architecture.

authorized users can access cloud platform data via mobile apps or the web browser.

B. HARDWARE IMPLEMENTATION

The designed IAQD consists of four functional components, power module, sensors module, MCU (microcontroller unit) controller module, and wireless module. The MCU controller collects temperature, humidity, CO2, and PM2.5 parameters, and stores data as the format of Modbus RTU protocol. Power module provides power for MCU, sensors and wireless module, with 5 V and 3.3 V, respectively.

1) SENSORS SELECTION

The proposed IAQD integrates PM2.5, CO_2, temperature and humidity sensors. Fig. 2 shows the sensors selected in this paper, and the detail parameters of these sensors are described in Table 2, which includes resolution, accuracy, range and interface to MCU. PMS5003 is a high-precision

TABLE 2. Basic parameters of the sensors used in this study.

Example Product	Parameter	Resolution	Accuracy	Range	Interface	Power
SHT30	Temperature	0.015 °C	±0.2 °C	-40~125 °C	I^2C	3.3 V
	Humidity	0.01 %RH	±2%	0-100 %RH	I^2C	3.3 V
PMS5003	PM2.5	1 μg/m^3	±10 μg/m^3	0-10000 μg/m^3	UART	5 V
S8 0053	CO_2	1 ppm	±40 ppm	400 to 2000 ppm	UART	5 V

FIGURE 2. Sensors and wireless module used in IAQD.

digital particulate concentration sensor made by Plantower company in China, which can be used to obtain the mass and quantity of suspended particulate matter (PM2.5) in the air and output in the form of a UART interface. PMS5003 sensor adopts laser scattering principle, which has higher precision compared to the ultra-red sensor, and can be easily used without calibration. The power consumption value is less than 100 mA in active mode and 200 μA in sleep mode. SHT30 is a new temperature and humidity sensor produced by Sensirion company in Switzerland, with an I^2C communication interface to MCU and a wide operating voltage range, suitable for various applications. The average power consumption is 4.8 μW. Finally, CO_2 sensor is S8 0053, which is made by SenseAir company in Sweden. The response time of S8 0053 is about 20 seconds and it has a very high measurement accuracy, with a long service life up to 15 years. The average power consumption is 18 mA. All these sensors adopted in this thesis can obtain high accuracy without calibration, and communicate to MCU via serial TTL interface, except SHT30, which is I^2C interface.

C. MCU MODULE

According to the requirements of sensor module and communication module, the MCU controller should have I^2C interface and at least three UART interfaces. We choose a 48-pin STM32F103C8T6 as microcontroller, which is a Cortex-M3 embedded 32-bit ARM, operating at 72 MHz frequency. The average power consumption is 25 mA, and there is a low power wake-up mode, which helps to save energy. This microcontroller provides one I^2C and three USART interfaces, which makes it suitable for this proposed IAQD. The basic circuit of MCU module includes reset circuit, crystal circuit and Joint Test Action Group (JTAG) circuit, which is used for development and debugging. The USART-1 is connected to PM2.5 sensor, USART-2 is connected to CO_2 sensor, and USART-3 is connected to the Zigbee wireless module.

1) ZIGBEE WIRELESS MODULE

Zigbee network is a mesh structure wireless sensor network (WSN), a network consisting of a Coordinator and many Routers or End-devices. All nodes in the network must have the same communication channel and the same PAN ID. The advantage of the Zigbee network is that it supports dynamic routing maintenance. When some nodes in the network break down, the system will automatically rediscover a new routing path to communicate. On the other hand, when a new node is added to the system, the system automatically updates the route without manual configuration. In addition, Zigbee has the characteristics of low speed, low power consumption, flexible automatic networking mode, plug-and-play. Furthermore, its large-scale network capacity can support a large number of online nodes, and has been widely used in smart home, environmental monitoring, building energy consumption monitoring and other fields. This article carries out multi-point monitoring in the home, and Zigbee meets the transmission network demand of the experiment.

The Zigbee wireless module selected in this paper is DRF1609H, which integrates TI latest Zigbee wireless chip CC2630 inside, and supports 200 levels of routing depth. Besides this, the module offers a software in computer and users can view the routing status of the whole network, as well as the signal strength of each node, which is very convenient for network debugging. The module size is 32 mm∗16 mm∗3 mm, and supply voltage is 3.3V. Its average power consumption is 25 mA, 18 mA in standby mode, 20 mA in receive mode and 200 mA in transmit mode. Furthermore, it supports serial transparent transmission for users, so that you only need to operate USART-3 of MCU to realize Zigbee wireless communication. The working time of the system is 30s, including 5s for data collection and 25s for data transmission. After many experiments, the average result shows that the energy consumption of the proposed system to complete a monitoring task is 0.38 mA·h.

The final prototype of the designed IAQD is shown in Fig. 3, which shows the top view, bottom view, inside and the whole prototype, respectively. The estimated cost of the hardware system is shown in Table 3, including the mentioned 3 types of sensors, Zigbee wireless modules, MCU modules and resistance capacitance (RC) elements, integrated circuit boards, and equipment shell. The total price of hardware including a single monitoring system is $47.2.

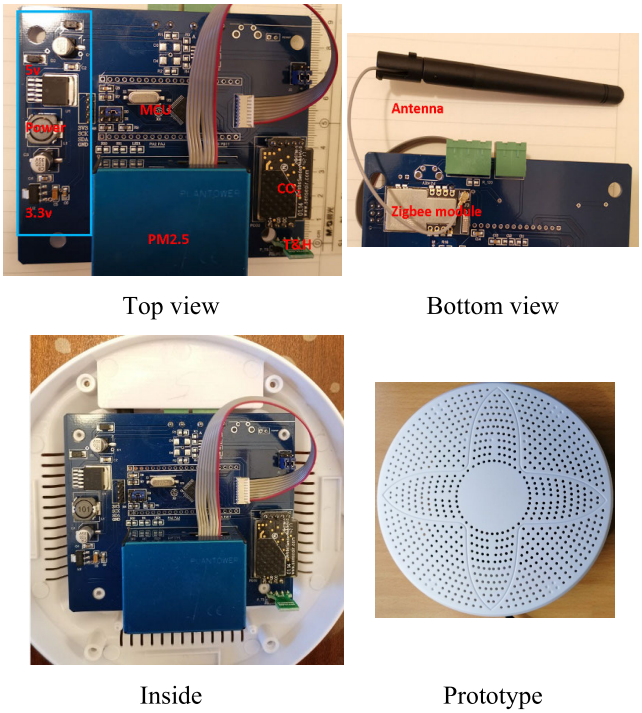

Top view Bottom view

Inside Prototype

FIGURE 3. The final prototype assembly.

TABLE 3. Hardware cost of a single monitoring system.

Material	Amount	Unit Price
SHT30 sensor	1	$0.7
S8 0053 sensor	1	$21.5
PMS5003 sensor	1	$10
Zigbee module	1	$7
MCU and RC elements	1	$3
Integrated circuit board	1	$2
Shell	1	$3
Total	-	$47.2

D. EMBEDDED SOFTWAR IN MCU

This section describes the embedded software design of IAQD that is required to take a measurement and store it in the memory as Modbus RTU format. Each IAQD has its unique address on the Modbus fieldbus. Fig. 4 shows the workflow of software, which consists of initialization module, collection module, package module, receiving and processing Modbus message module, sending module, configuration module and watchdog (WDG) module.

1) MODBUS PROTOCOL

Modbus is a field bus protocol in the field of industrial communication, which has been widely used in various industrial

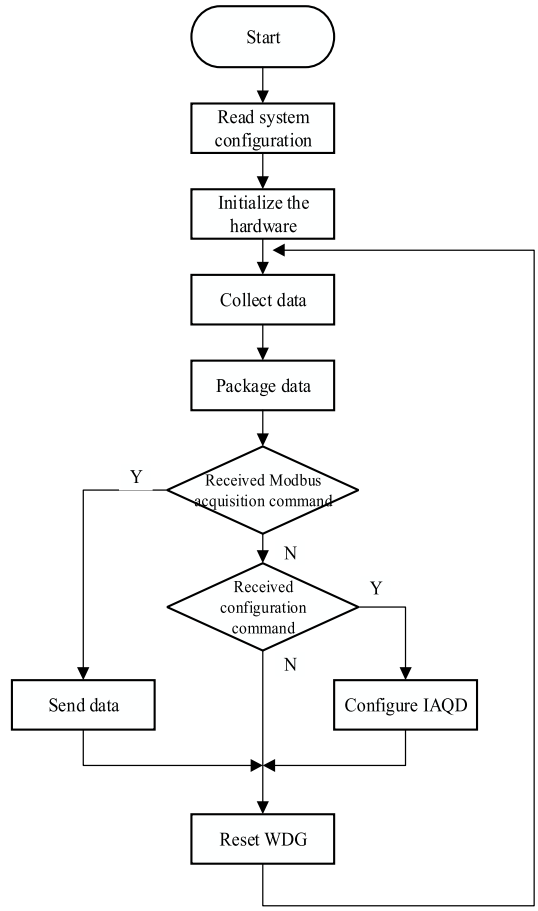

FIGURE 4. Workflow of the IAQD.

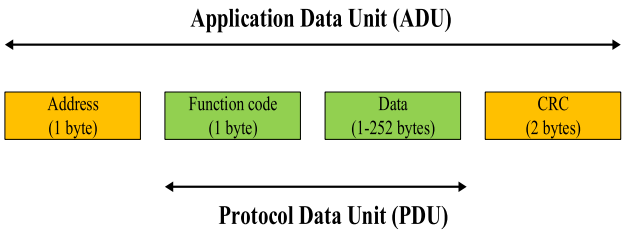

FIGURE 5. The structure of data frame in Modbus-RTU.

occasions since 1979 [25]. Fig. 5 shows the structure of the data frame in Modbus RTU, including four message structures: address, function code, data and CRC (cyclic redundancy check) [26]. The first three fields contain the necessary information for Modbus transactions, while the fourth field corresponds to a 16-bit CRC calculation to detect errors.

In this IAQD, all the data sensor packets are stored as format of Modbus RTU. Table 4 describes the registers of these parameters. The range of a word variable is 0-65535, covering the range of PM2.5 and CO_2. Since the Modbus packet is a word variable, and cannot express the decimal part. For temperature and humidity, in order to improve the measurement accuracy, the data is stored after multiplied by ten. When the cloud platform receives the data, divides it by ten to get the original value.

TABLE 4. Modbus RTU registers of IAQD.

Parameter	Register	Type	Note
PM2.5	0x01	unsigned word	original
CO_2	0x02	unsigned word	original
Temperature	0x03	signed word	10 times
Humidity	0x04	unsigned word	10 times

2) INITIALIZATION MODULE

This process includes the initialization of system clock, UARTs, I^2C interface, flash memory. There are three UARTs of STM32: the first UART is used to communicate with PM2.5 sensor; the second UART is used to communicate with CO_2 sensor; the third channel is used to communicate with DTU (data transfer unit). The parameters of serial port configuration include baud rate, start bit, stop bit and check bit, and the corresponding configuration parameters in this study are 9600, N, 8, 1. I^2C interface is used to communicate with temperature/humidity.

3) IAQD CONFIGURATION MODULE

Each IAQD connected to Modbus bus needs to have a unique ID, and the address cannot be repeated. Otherwise, there will be a bus communication failure and data cannot be read. Under the default condition, all IAQD communication parameters are 9600, N, 8, 1, and the communication address is 1. When the address is needed to be modified, the following message can be sent.

$$FF\ AA\ 55\ 22\ 00\ 01\ 00\ xx\ CRC$$

where, "FF AA 55 22"is a synchronous frame signal. When STM32 detects the signal, it will know that this is a configuration message, and configure the current IAQD according to the following information. "00 01" is the register corresponding to address modification, and "00 xx" is the target address to be modified. The Modbus filed bus allows up to 256 nodes on the bus in the same time, and there are seven IAQDs in this proposed monitoring system.

4) DATA ACQUISITION MODULE

The microcontroller collects the temperature and humidity data from SHT31 through I^2C bus as 16-bit values (unsigned integer). These values are already linearized and compensated for temperature and supply voltage effects. Converting those raw values into a physical scale can be achieved using the following formulas [27].

Relative humidity conversion formula (result in %RH):

$$RH = 100\frac{S_{RH}}{2^{16}-1} \tag{1}$$

where, S_{RH} denotes the raw sensor outputs of humidity.

Temperature conversion formula (result in °C):

$$T = 175\frac{S_T}{2^{16}} - 45 \tag{2}$$

where, S_T denotes the raw sensor outputs of temperature.

TABLE 5. Host protocol of PMS5003.

Start (2-bytes)	Command (1-byte)	Data1 (1-byte)	Data2 (1-byte)	Verify (2-bytes)
0x424D	CMD	DATH	DATAL	LRC

PMS5003 communicates with microcontroller through TTL serial port, and the transport protocol of host is shown in Table 5. By default, PMS5003 works in an active state, and sends a data packet every second after power on. PMS5003 has two working states, low power consumption state and working state. After entering the low power consumption state, it can save the energy consumption of the sensor, and can be used in low-power monitoring occasions. After entering the working state, it can be divided into two modes: active sending mode, which sends a data message every second, and the other is passive mode, which returns the data message after receiving the acquisition command sent by microcontroller. In this study, we select the passive mode, and PMS5003 is configured to work in the passive mode during initialization.

S8 0053 provides two data interaction interface, serial communication and PWM. In this study we choose serial communication and the process of data acquisition is similar to PM2.5 sensor, which will not be discussed.

5) WATCHDOG SERVICE

The watchdog service is a mechanism for detecting and recovering when STM32 failures. STM32 has a built-in watchdog module. When the watchdog service is enabled, a counter counts down from some initial value that can be configured. An interrupt signal will be generated, if the counter reaches zero, and makes the microcontroller reset. When developing the software, you need to reinitialize the watchdog module at a suitable location to prevent software from crashing.

E. MONITORING SYSTEM IN CLOUD PLATFORM

As aforementioned, authorized end users can access the air quality monitoring system in the form of website or mobile APP. Our website software is developed using web page configuration tool, the development of cloud platform software can be completed quickly finished by what you see is what you get (WYSIWYG) approach. Fig. 6-(a) illustrate the GUI interfaces of the website and the mobile APP, respectively. Through the display applications, the air quality information can be shown in real-time, e.g.

- Real-time indoor air quality data.
- IAQ trend of in a day, week or time period by user defined.
- IAQ historical data query and export function, shown as in Fig. 6-(b).
- Setting of alarm values.
- Managing user access permissions.

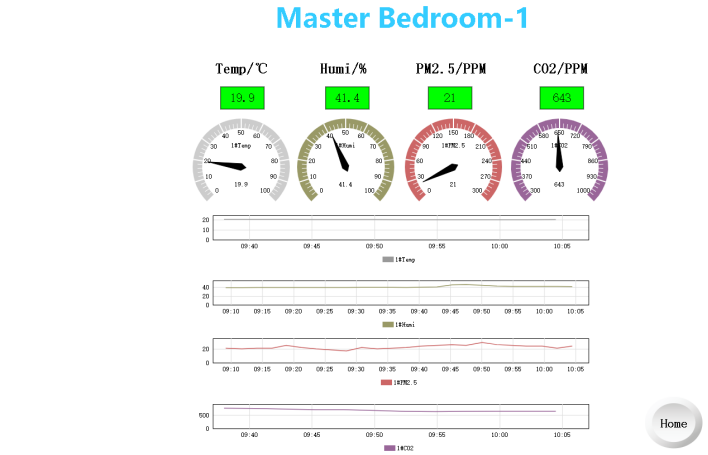

(a) distributed monitoring page

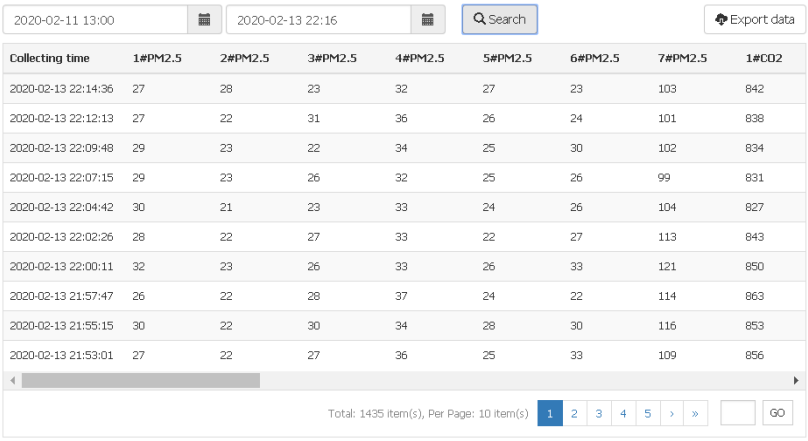

(b) historical data report

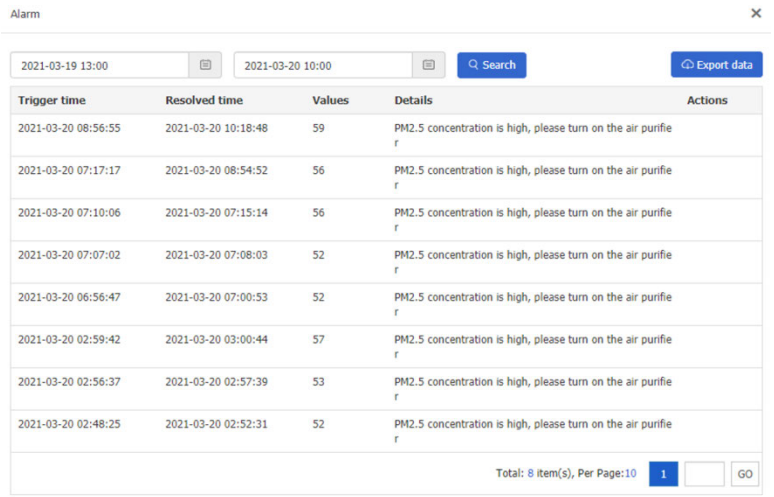

(c) monitoring alarm function

FIGURE 6. Monitoring system on the cloud platform.

The real-time monitoring software of the cloud platform of the system is developed by the configuration of WYSIWYG, and developer can complete the monitoring system development task by building blocks, and the modular development method can improve the efficiency of the system [28]. As shown in Fig. 6-(a), by clicking on the digital label edit edging in the graph, you can enter the detailed monitoring data of the corresponding room. In addition, the main interface also gives the monitoring real-time graph of 4 measured variables, which is convenient for the overall control of the

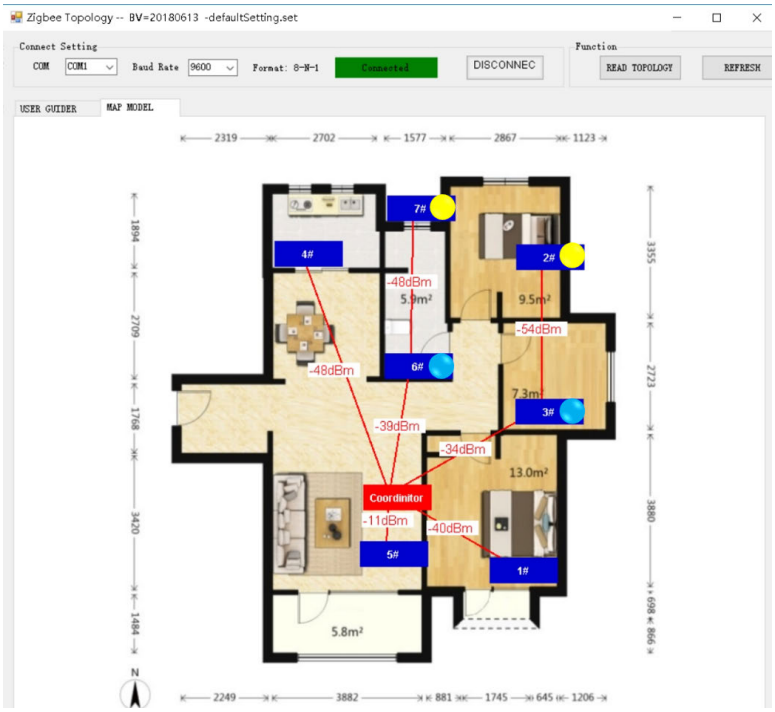

FIGURE 7. Deployment of zigbee network and location of IAQDs.

system. Fig. 6-(a) also gives a monitoring chart of the master bedroom, showing the monitoring data in real time in the form of dashboard and values, which can show fluctuations of the past 6 hours through the graph, and clicking on the ''home'' button in the lower right corner to return to the main interface.

The cloud platform monitoring system provides data export capability, which enables the export of historical data in the form of CSV reports for in-depth data analysis and mining. As shown in Fig. 6-(b), data is exported in a 1-day, 1-week, 1-month period or user-defined time period. Compared with the traditional local monitoring system Client/Server (CS) architecture, the current popular cloud platform monitoring system can provide cross-platform Browser/Server (BS) access, authorized users can access the monitoring system from anytime, anywhere. By setting the alarm trigger threshold, we can grasp whether the measured parameters are in a safe running state. Through this module, we can see detailed alarm information, including alarm time, alarm equipment, alarm parameters and alarm details, as shown in Fig. 6-(c). The information in the alarm details can be used to remind users to take measures to reduce the harm caused by environmental quality. Especially the alarm push function of the mobile side, which provides the real-time and robustness of the system.

IV. EXPERIMENTAL RESULTS AND ANALYSIS

In this section, we will focus on the evaluation of performances of the proposed IAQD system. The performance of communication using Zigbee modules is evaluated indoor in a residential apartment in Dalian, China (coordinates N38.5°, E121.29°). To demonstrate the performance of presented IAQD system, we deployed seven monitoring points in the target apartment, and conducted indoor and outdoor sampling from Jan-18 to Feb-17 2020. During the winter measurement period, the target apartment adopts geothermal heating instead of radiators or air conditioners, which ensures that the temperature distribution of each room is uniform.

A. IAQD MONITORING POINTS LAYOUT

The layout diagram of apartment is shown in Fig. 7, with an area of 124 m^2. We deployed six IAQDs indoor and one IAQD outside of the apartment. The monitoring points marked with numbers could be used as codes of monitoring rooms. 1# at master room, 2# at second room, 3# at activity room, 4# at kitchen, 5# at living room, 6# at bathroom and 7# at outside. Each IAQD has a Zigbee communication module, and the coordinator of WSN is located in the living room. The detail placements of each IAQD and coordinator are shown in Fig. 7. The 1#, 2#, 3#, 6# IAQD are on the bedside cabinet, about 70cm above floor. 5# is on the TV cabinet, about 40 cm above floor, and the coordinator is located in the TV cabinet. The 4# is on the windowsill of kitchen, about 60cm above floor. Finally, the 7# is on the air conditioner at the north side of the apartment, where there's no direct sunlight to the IAQD during the day.

The topology of the Zigbee network is shown in Fig. 7, with seven IAQD modules connected directly or indirectly to the coordinator. The signal strength of each Zigbee node can be read out through debugging software as shown in Fig. 7. The signal quality of 5#, which is closest to the coordinator, is better than others. The IAQDs far from the coordinator are transmitted through the router node (3# and 6#), such as 2# is

connected to the coordinator via 3# and 7# is located outdoors through the 6#, respectively. The IAQD located on the second bedroom, has the worst signal quality of all the seven nodes.

B. PACKET LOSS ANALYSIS

The data collector sends collection packet (8 Bytes) via Modbus protocol as following format:

01 03 00 00 00 04 44 09

where, 01 is the address of 1# IAQD, 03 is the function code of reading, 00 00 is the start address of register, 00 04 is the length of reading register, and 44 09 is the CRC check code. The address of IAQD is changing from 01 to 07 in each reading cycle. The collection packet is sent via Zigbee coordinator, and all nodes in the network can receive it, but only the matched IAQD will reply a data packet (13 Bytes) to the collector. If the data collector does not receive a return data message of the corresponding IAQD, it will send three acquisition instructions in a row. Furthermore, if there is still no reply for three times, a packet drop occurs. The drop rate for each node can be obtained by dividing the total number of messages sent by the return message received by the data collector.

Fig. 8 shows the packet loss ratio (PLR) of seven IAQDs. From this figure, we can see that PLR of 2# in the second bedroom is the largest, with a value of 8.24%. There are at least 2 walls obstacle between this point and the coordinator, as shown in Fig. 7, resulting in a significant attenuation of the wireless signal. On the other hand, the PLRs of 5# in the living room and 4# in the kitchen are very small, less than 0.1%. This is because there is no obvious obstacle between these two points and the coordinator. In the case of the line-of-sight transmission, and the transmission distance is not far, the PLR of Zigbee is small. The PLR of 1# point in the master bedroom is slightly higher than the PLRs of 4# and 5#, with the value of 0.14%. The PLRs of 3#, 6# and 7# are greater than 1#, but still less than 2%. The 7# at outside of apartment has the furthest distance from the coordinator, but PLR is less than 2# in the second bedroom. This situation illustrates that, compared with distance, obstacle blocking has a greater impact on the loss of wireless signals.

C. MEASUREMENT RESULTS AND ANALYSIS

1) OVERALL TREND ANALYSIS

The overall PM2.5 quality monitoring of each room for a month is shown in Fig.9. From this figure, we can see that, for most of the time, the concentration of PM2.5 outdoors is significantly higher than indoor, except for a few values occasionally measured at the 4# point in the kitchen. Sudden high measurements are caused by fumes cooking in the kitchen, and most of these points occur during lunch or dinner time. Furthermore, from the enlarge figure (marked "A"), the PM2.5 concentration of 4# is also higher than the values in the other rooms in addition to the cooking time period. This is due to the placement of the 4# point at the kitchen

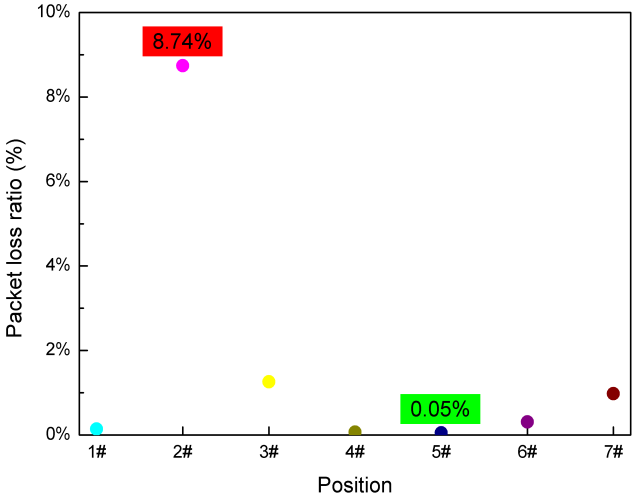

FIGURE 8. Packet loss ratio of different IAQDs.

window closest to the outdoors compared with other monitoring points, and are vulnerable to outdoor environments.

Table 6 describes the statistical analysis results of PM2.5, CO_2, temperature, and humidity. From the table, it can be seen that 4# in the kitchen has the highest value, 1091 $\mu g/m^3$. If the concentration of PM2.5 exceeds 250 $\mu g/m^3$, it will be seriously harmful to the human body [9]. The smoke of cooking in the kitchen is one of the main factors that causes lung cancer. Further, the average PM2.5 in the kitchen is 52.2 $\mu g/m^3$, 37% higher than average of other rooms. The average concentration of PM2.5 outdoors is 86.6 $\mu g/m^3$, 65.9% higher than the average of kitchen and 127.9% higher than the average of several other rooms.

Fig. 10 describes the change curve of CO_2. It can be clearly seen that the CO_2 concentration at the 7# outdoors is small, with an average value 423 ppm, and maximum is 550 ppm. Other indoor monitoring points fluctuate violently, and the fluctuation of CO_2 is correlated with the trajectory of human activity indoors. Similar to Fig. 9, the concentration of CO_2 increased significantly when people were active in the kitchen. Furthermore, from the enlarged plot of point B in the Fig. 10, it can be seen that during the sleep time in the night, the monitoring values of CO_2 in the bedrooms are climbing gradually. The maximum concentration of CO_2 in the master bedroom (two adults) reached 1100 ppm, and the concentration of CO_2 in the second bedroom (one seven-years-old child) reached 950 ppm, while the values in other rooms in the same section was relatively lower.

From Table 6, it can be concluded that, the maximum of CO_2 is still in the kitchen. The area of kitchen is smaller than bedrooms, and the value of CO_2 would increase rapidly. In the indoor environment, the average CO_2 of the master bedroom is the highest, 862 ppm, and the average CO_2 of the living room is the lowest, 672 ppm. Compared with other rooms, the living room area is large, and the concentration of CO_2 diffusion is fast, while other rooms, such as kitchen, bathroom is small, and the CO_2 concentration diffusion is slower.

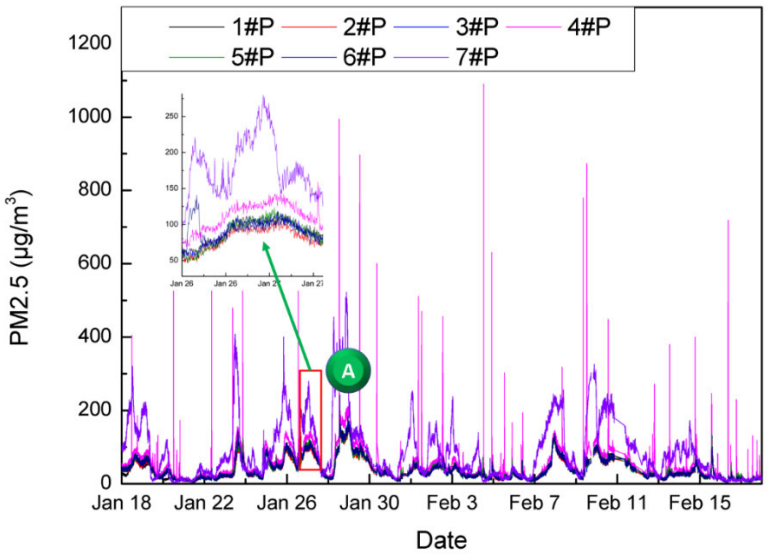

FIGURE 9. PM2.5 quality monitoring for a month.

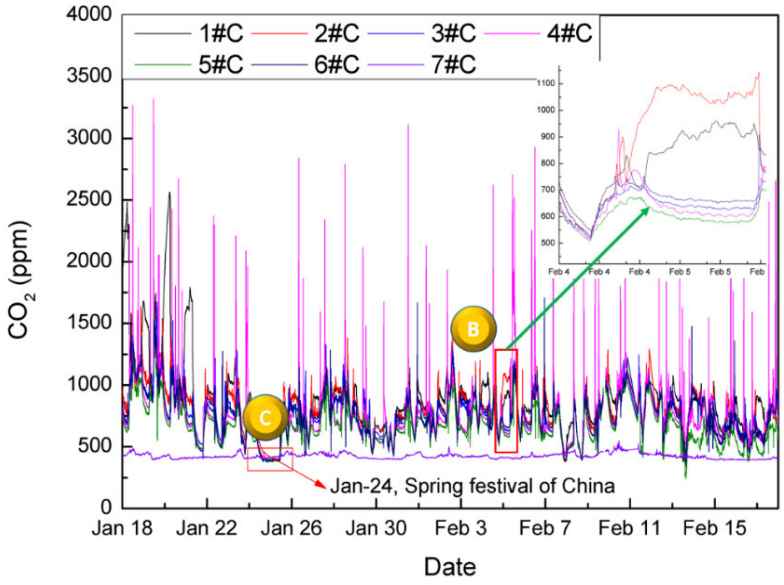

FIGURE 10. CO_2 quality monitoring for a month.

There were no people at home on January 24, which is China's traditional festival, Spring Festival, and the CO_2 concentration of each room was balanced, and maintained at a low level, as shown in point C in Fig. 10.

The monitoring period of this paper is in winter, with a minimum outdoor temperature of −14.3°, a maximum temperature of 12.6 °, and an average temperature of −1.2°. The apartments are heated with geothermal heating, and the temperature of each room is relatively uniform. The standard temperature of winter heating in China is 18 °, and the temperature of heating in this apartment meets the user's requirements.

Fig. 11 describes the temperature changing curves, which appears a clear layering trend. The master bedroom and living room locate in the south-direction, with a longer period of direct sunlight during the day and have a significantly higher temperature than other rooms. The activity room is located on the east side and can receive light from the sun in the morning, so that the temperature is slightly higher than the second bedroom on the north side. The statistics of temperature values in Table 6 show that, the average temperature of master bedroom is 21.6 °, and 18.4 ° in the second bedroom, which indicates that the temperature of room in the south is 17.3% higher than the room in the north. The 4# IAQD in the kitchen is placed on the window, which has the lowest average temperature of all the rooms, and the fluctuation is relatively violent, consistent with the trend of external ambient temperature.

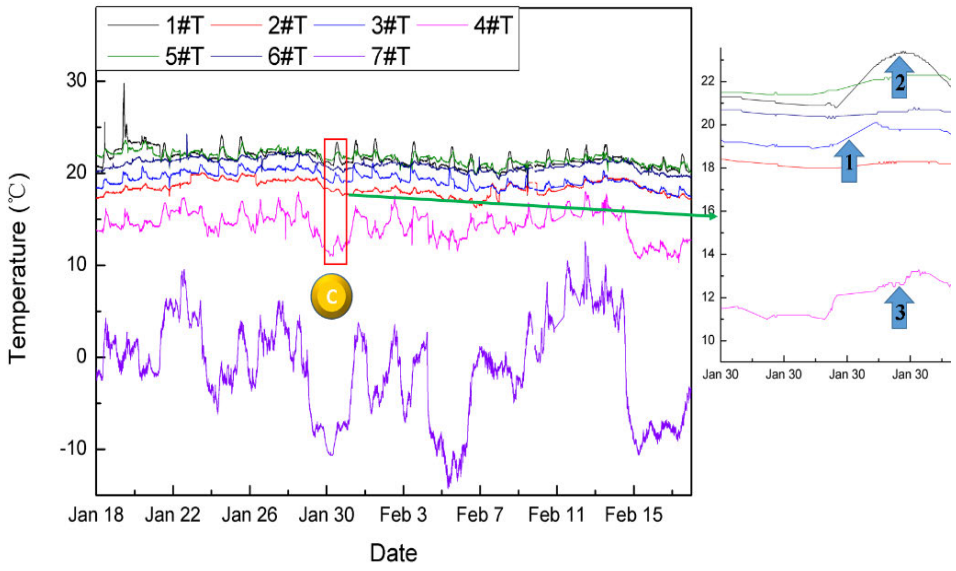

FIGURE 11. Temperature monitoring for a month.

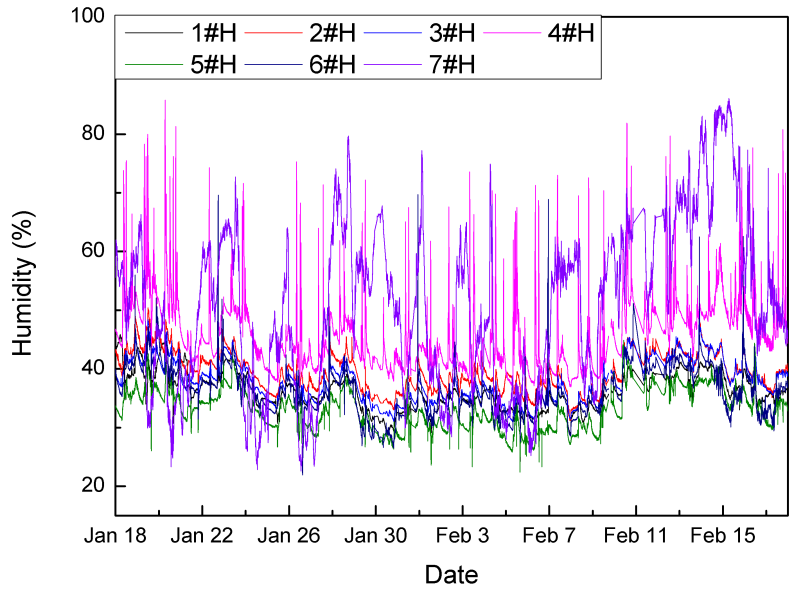

FIGURE 12. Humidity monitoring for a month.

From the enlarged point C in the Fig. 11, it can be seen that when the day is sunny, the temperature of the activity room first rises, then the temperature of the master bedroom begins to rise, and the temperature of the kitchen rises as the external environment rises.

Fig. 12 shows the changing curves of humidity, and from the overall view, the change of indoor humidity follows the trend of outdoor humidity. The average humidity shown in Table 6 infers that the humidity value in the winter of each room is low, and the average humidity of the master bedroom is 36.2% and the humidity value of the second bedroom is 39.6%, which are below the best relative humidity for human, 45% to 60%. When the humidity is less than 40%, the flue movement on the respiratory mucosa of the nose and lungs weakens, and viruses and bacteria can easily attach to the mucous membrane, causing respiratory diseases such as coughing [29]. In addition, when the humidity is low, the rate of reproduction of infectious bacteria such as influenza viruses will accelerate. Meanwhile, asthma and other allergic diseases are also prone to occur [30].

2) ANALYSIS OF THE IMPACT OF WINDOW OPENING

As can be seen from Table 6, the maximum CO_2 concentration of the master bedroom is 2566 ppm and the maximum value of the second bedroom is 1638 ppm. Human will feel uncomfortable if the concentration of CO_2 exceeds 1500 ppm, and long-term inhalation of high concentration of CO_2 will cause the disorder of human body's biological

TABLE 6. Indoor air quality monitoring statistics.

Type		1#	2#	3#	4#	5#	6#	7#
PM2.5 ($\mu g/m^3$)	Max	176	157	166	**1091**	182	242	***523***
	Min	3	2	3	4	3	2	***2***
	Avg	39.4	37.3	38.2	**52.2**	37.2	37.6	***86.6***
CO_2 (ppm)	Max	2566	1638	1674	**3318**	1576	1709	***550***
	Min	341	370	369	366	342	371	***385***
	Avg	862	794	769	760	672	749	***423***
Temp (°C)	Max	**28.8**	20.1	21.1	18	23.6	24.3	***12.6***
	Min	17.6	16.3	17.4	10.3	19.9	19.4	***-14.3***
	Avg	21.6	18.4	19.3	14.4	21.7	20.9	***-1.2***
Humi (%)	Max	45.9	51.1	50.5	**85.8**	44.9	69.7	***86.1***
	Min	24.2	30.1	29.3	28.7	22.4	21.9	***22.6***
	Avg	36.2	39.6	38.1	45.9	33.2	36.4	***50.5***

clock. The high concentration of CO_2 can inhibit the respiratory center of the person, which also has a paralyzing effect on the respiratory center. It is easy to feel brain fatigue, reduced productivity, and damage to human health, if you stay in a high concentration of CO_2 for a long time. The window ventilation allows fresh air from the outside to enter the inside rooms, and reduces the CO_2 concentration. However, in the winter of northern China, the PM2.5 concentration of outdoor is very high due to the effects of central heating, which is also harmful to the human body. Therefore, indoor ventilation needs to choose the right time.

Fig. 13 describes the effect of ventilation on indoor PM2.5 and CO_2 concentration on Jan-22 and Jan-28. As shown in point D in Fig. 13-(a), after opening the window, the CO_2 concentration in the master bedroom and living room quickly dropped from 1000 ppm to 600 ppm. At the same time, the corresponding PM2.5 concentration increased slightly, from 20 $\mu g/m^3$ to 40 $\mu g/m^3$. Due to the excellent outdoor air quality, the air in all rooms becomes fresh and comfortable after ventilation.

Fig. 13-(b) shows twice ventilation effects on Jan-28. It can be seen that the outdoor PM2.5 concentration has reached 450 $\mu g/m^3$, at a serious pollution state. The first ventilation happened at 8 o'clock, and resulted in a slight increase in the concentration of PM2.5 indoor from 50 $\mu g/m^3$ to 100 $\mu g/m^3$, as shown in point E in Fig. 13-(b). The second ventilation occurred at about 13:00 and caused the indoor PM2.5 concentration to rise significantly, from 100 $\mu g/m^3$ to 180 $\mu g/m^3$, resulting in a moderate pollution state of indoor air quality, as shown in point F in Fig. 13-(b). On the other hand, the CO_2 concentration of these two points were also correspondingly reduced, but in exchange for PM2.5 from good state to moderate pollution, which is obviously not worth the loss.

3) ANALYSIS OF THE IMPACT OF WINDOW OPENING

As depicted in Fig. 10, the CO_2 concentration of the master and second bedrooms will rise to a high level of more

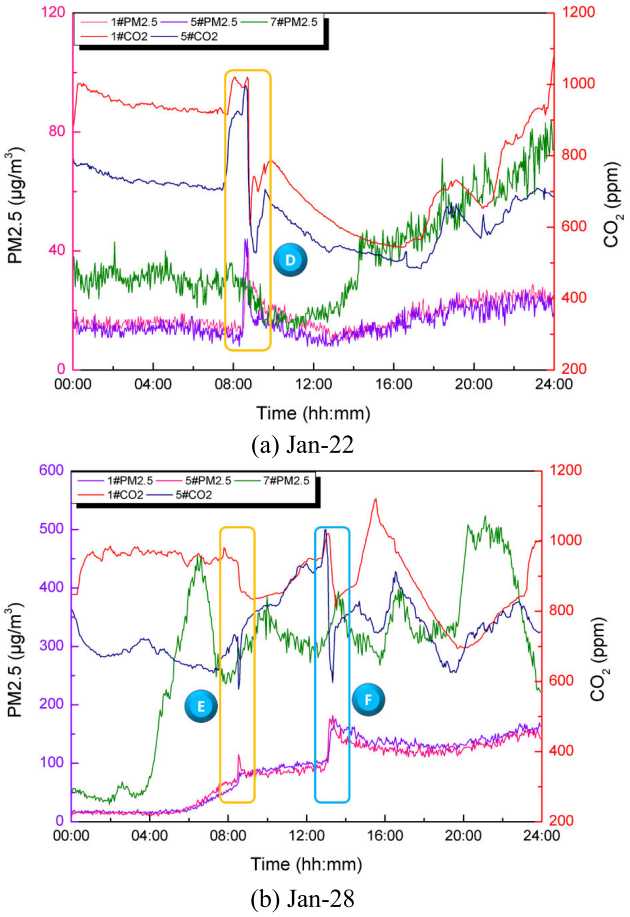

FIGURE 13. Effects of window opening on indoor air quality.

than 1000 ppm, during the sleep period at night. To study the effect of closing and opening door of bedroom on the concentration of CO_2 at sleeping period indoors, we did two sets of comparative tests. Fig. 14 shows the test results from Jan-20 to Jan-22. The master bedroom closed door to sleep on Jan-20 and Jan-21, and opened the door to sleep on Jan-22 and Jan-23. On the other hand, the second bedroom kept the door open while sleeping time during the experiment.

As shown in point G of Fig. 14, the concentration of CO_2 rose rapidly when the master bedroom door is closed, and the value is much higher than the concentration of the second bedroom and living room. The highest values of CO_2 of master bedroom reached 2566 ppm and 1750 ppm on Jan-20 and Jan-21, respectively. The average concentrations of CO_2 were 1987 ppm and 1589 ppm from 21:30 to 7:30 of these two days, respectively. In addition, the average concentrations of CO_2 were 91.9% and 73.3% higher than the second bedroom respectively. However, when the master bedroom also opened the door to sleep on Jan-22 and Jan-23, as shown in point H in Fig. 14, the difference in CO_2 concentration between the two rooms was not very obvious.

The point I in Fig. 14 indicated that during the 21:00-22:00 period, the CO_2 concentration of the second bedroom rose steeply, then fell back rapidly, and then began

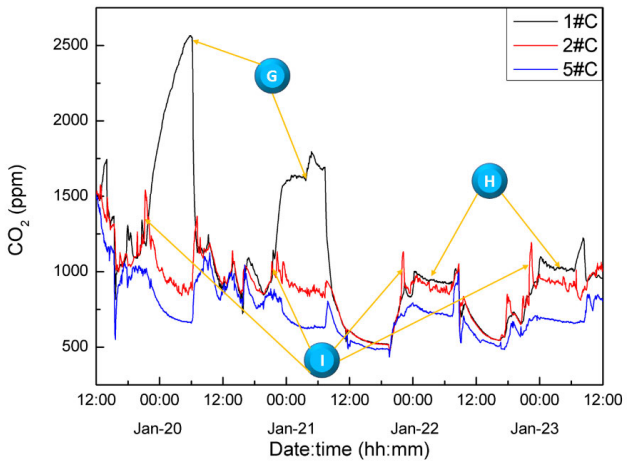

FIGURE 14. Statistical analysis of monitoring data for a day.

to decline steadily or slowly. This was due to ''story time'' when father or mother told the child a bedtime story every night. Again, the results show that the change of indoor CO_2 concentration is closely related to the human trajectory of action.

V. CONCLUSION

This paper presented an indoor air quality detector (IAQD) system made up of a Zigbee wireless network, which enables monitoring of PM2.5, CO_2, temperature and humidity simultaneously. Furthermore, we put forward a multi-point monitoring system in a residential building based on the Internet of Things (IoT). Compared with previous studies, we have deployed multiple monitoring points in the building to more realistically reflect the air quality in the building. By analyzing the continuous measurement data of the system for one month in winter, the conclusions are as follows:

- For Zigbee wireless network, the wireless signal quality is greatly affected by concrete walls. After crossing over two walls, the packet loss ratio will be more than 8%.
- When people cook in the kitchen, the concentration of PM2.5 will be 10 times higher than usual, and seriously hurt human's health.
- The concentration of CO_2 in the room is high due to the reduced frequency of opening windows in the winter, especially when sleeping at night, the CO_2 concentration in the bedroom will exceed 1000 ppm. Furthermore, the concentration of CO_2 will reach 2500 ppm with the door closed at night. In addition, we should pay attention to observe whether the outdoor PM2.5 concentration is suitable for ventilation during the daytime.
- The average north bedroom temperature is about 3 degrees lower than in the south, and the humidity in all rooms is dry, requiring special attention to the occurrence of colds or respiratory diseases.

In the future, we will improve the Zigbee wireless sensor network and consider switching to LoRa communication to enhance the penetration of wireless signals indoors and reduce PLR. Additionally, during the experiment, we found that the changes of CO_2 concentration have a strong relationship with the human action trajectory, and the changes can be studied to identify indoor occupancy and tracked the activity path of personnel through the concentration of CO_2. On the other hand, long-term monitoring of different types of buildings is also considered to provide a more in-depth study of indoor air quality.

REFERENCES

[1] A. de Nazelle, E. Seto, D. Donaire-Gonzalez, M. Mendez, J. Matamala, M. J. Nieuwenhuijsen, and M. Jerrett, ''Improving estimates of air pollution exposure through ubiquitous sensing technologies,'' *Environ. Pollut.*, vol. 176, pp. 92–99, May 2013.

[2] S. C. Lee, S. Lam, and H. K. Fai, ''Characterization of VOCs, ozone, and PM_{10} emissions from office equipment in an environmental chamber,'' *Building Environ.*, vol. 36, no. 7, pp. 837–842, Aug. 2001.

[3] J. He, L. Xu, P. Wang, and Q. Wang, ''A high precise E-nose for daily indoor air quality monitoring in living environment,'' *Integration*, vol. 58, pp. 286–294, Jun. 2017.

[4] C. Peng, K. Qian, and C. Wang, ''Design and application of a VOC-monitoring system based on a ZigBee wireless sensor network,'' *IEEE Sensors J.*, vol. 15, no. 4, pp. 2255–2268, Apr. 2015.

[5] T.-C. Yu, C.-C. Lin, C.-C. Chen, W.-L. Lee, R.-G. Lee, C.-H. Tseng, and S.-P. Liu, ''Wireless sensor networks for indoor air quality monitoring,'' *Med. Eng. Phys.*, vol. 35, no. 2, pp. 231–235, Feb. 2013.

[6] S. C. Anenberg, L. W. Horowitz, D. Q. Tong, and J. J. West, ''An estimate of the global burden of anthropogenic ozone and fine particulate matter on premature human mortality using atmospheric modeling,'' *Environ. Health Perspect.*, vol. 118, no. 9, pp. 1189–1195, Sep. 2010.

[7] S. C. Folea and G. Mois, ''A low-power wireless sensor for online ambient monitoring,'' *IEEE Sensors J.*, vol. 15, no. 2, pp. 742–749, Feb. 2015.

[8] X. Liu and X. Zhang, ''NOMA-based resource allocation for cluster-based cognitive industrial Internet of Things,'' *IEEE Trans. Ind. Informat.*, vol. 16, no. 8, pp. 5379–5388, Aug. 2020.

[9] X. Liu, X. B. Zhai, W. Lu, and C. Wu, ''QoS-guarantee resource allocation for multibeam satellite industrial Internet of Things with NOMA,'' *IEEE Trans. Ind. Informat.*, vol. 17, no. 3, pp. 2052–2061, Mar. 2021.

[10] X. Liu and X. Zhang, ''Rate and energy efficiency improvements for 5G-based IoT with simultaneous transfer,'' *IEEE Internet Things J.*, vol. 6, no. 4, pp. 5971–5980, Aug. 2019.

[11] O. A. Postolache, J. M. D. Pereira, and P. M. B. S. Girao, ''Smart sensors network for air quality monitoring applications,'' *IEEE Trans. Instrum. Meas.*, vol. 58, no. 9, pp. 3253–3262, Sep. 2009.

[12] S. Sun, X. Zheng, J. Villalba-Díez, and J. Ordieres-Meré, ''Indoor air-quality data-monitoring system: Long-term monitoring benefits,'' *Sensors*, vol. 19, no. 19, p. 4157, Sep. 2019.

[13] H. Zhang, R. Srinivasan, and V. Ganesan, ''Low cost, multi-pollutant sensing system using raspberry pi for indoor air quality monitoring,'' *Sustainability*, vol. 13, no. 1, p. 370, Jan. 2021.

[14] P. Spachos and D. Hatzinakos, ''Real-time indoor carbon dioxide monitoring through cognitive wireless sensor networks,'' *IEEE Sensors J.*, vol. 16, no. 2, pp. 506–514, Jan. 2016.

[15] G. Marques, C. R. Ferreira, and R. Pitarma, ''Indoor air quality assessment using a CO2 monitoring system based on Internet of Things,'' *J. Med. Syst.*, vol. 43, no. 3, p. 67, Feb. 2019.

[16] M. F. M. Firdhous, B. H. Sudantha, and P. M. Karunaratne, ''IoT enabled proactive indoor air quality monitoring system for sustainable health management,'' in *Proc. ICCCT*, Chennai, India, Feb. 2017, pp. 216–221.

[17] L. Bai, Z. He, C. Li, and Z. Chen, ''Investigation of yearly indoor/outdoor $PM_{2.5}$ levels in the perspectives of health impacts and air pollution control: Case study in Changchun, in the northeast of China,'' *Sustain. Cities Soc.*, vol. 53, Feb. 2020, Art. no. 101871.

[18] M. Benammar, A. Abdaoui, S. Ahmad, F. Touati, and A. Kadri, ''A modular IoT platform for real-time indoor air quality monitoring,'' *Sensors*, vol. 18, no. 2, p. 581, Feb. 2018.

[19] N. Q. Pham, V. P. Rachim, and W.-Y. Chung, ''EMI-free bidirectional real-time indoor environment monitoring system,'' *IEEE Access*, vol. 7, pp. 5714–5722, 2019.

[20] A. Chamseddine, I. Alameddine, M. Hatzopoulou, and M. El-Fadel, "Seasonal variation of air quality in hospitals with indoor–outdoor correlations," *Building Environ.*, vol. 148, pp. 689–700, Jan. 2019.
[21] R. M. Nica, T. Hapurne, A. I. Dumitrascu, I. Bliuc, and C. Avram, "Proposal for a small two-story living room house based on air-quality monitoring," *Procedia Manuf.*, vol. 22, pp. 268–273, Jan. 2018.
[22] P. K. Cheung and C. Y. Jim, "Indoor air quality in substandard housing in hong kong," *Sustain. Cities Soc.*, vol. 48, Jul. 2019, Art. no. 101583.
[23] E. Svertoka, M. Bălănescu, G. Suciu, A. Pasat, and A. Drosu, "Decision support algorithm based on the concentrations of air pollutants visualization," *Sensors*, vol. 20, no. 20, p. 5931, Oct. 2020.
[24] B. D. Burghele, M. Botoş, S. Beldean-Galea, A. Cucoş, T. Catalina, T. Dicu, G. Dobrei, Ş. Florică, A. Istrate, A. Lupulescu, M. Moldovan, D. Niţă, B. Papp, I. Pap, K. Szacsvai, C. Sainz, A. Tunyagi, and A. Ţenter, "Comprehensive survey on radon mitigation and indoor air quality in energy efficient buildings from Romania," *Sci. Total Environ.*, vol. 751, Jan. 2021, Art. no. 141858.
[25] S. Figueroa-Lorenzo, J. Añorga, and Arrizabalaga, "A role-based access control model in modbus SCADA Systems. A centralized model approach," *Sensors*, vol. 19, no. 20, p. 4455, Oct. 2019.
[26] C. Urrea and C. Morales, "Enhancing modbus-RTU communications for smart metering in building energy management systems," *Secur. Commun. Netw.*, vol. 2019, pp. 1–8, Nov. 2019.
[27] *Conversion Formula of Values*. Accessed: May 20, 2020. [Online]. Available: https://www.sensirion.com/fileadmin/user_upload/customers/sensirion/Dokumente/2_Humidity_Sensors/Datasheets/Sensirion_Humidity_Sensors_SHT3x_Datasheet_digital.pdf
[28] L. Zhao, W. Wu, and S. Li, "Design and implementation of an IoT-based indoor air quality detector with multiple communication interfaces," *IEEE Internet Things J.*, vol. 6, no. 6, pp. 9621–9632, Dec. 2019.
[29] E. Piecková, "Indoor microbial aerosol and its health effects: Microbial exposure in public buildings–viruses, bacteria, and fungi," in *Exposure to Microbiological Agents in Indoor and Occupational Environments*. Oct. 2017, pp. 237–252.
[30] P. Wolkoff, "Indoor air humidity, air quality, and health—An overview," *Int. J. Hygiene Environ. Health*, vol. 221, no. 3, pp. 376–390, Apr. 2018.

ZHIBIN LIU received the Ph.D. degree in heating gas ventilation and air conditioning engineering from the Dalian University of Technology, in 2014. He is currently a Teacher with the College of Civil Engineering, Dalian Minzu University, Dalian, China. His current research interests include building energy-saving technology, and waste heat recovery technology and equipment.

GUANGWEN WANG was born in Shandong, China. He received the B.S. degree in automation from Northeast Forestry University, Harbin, Heilongjiang, in 2019. He is currently pursuing the master's degree with the School of Control Science and Engineering, Dalian University of Technology. His current research interests include the Internet of Things, embedded systems, and building energy information systems.

LIANG ZHAO was born in Harbin, China. He received the B.S. and M.S. degrees in electronic information engineering and the Ph.D. degree in heating gas ventilation and air conditioning engineering from the Dalian University of Technology, Dalian, Liaoning, in 2007, 2009, and 2014, respectively. He is currently an Associate Professor with the School of Control Science and Engineering, Dalian University of Technology. His current research interests include the Internet of Things and applications to embedded systems, and building energy information systems.

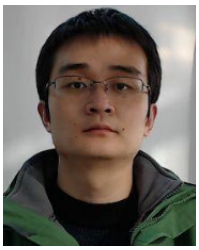

GUANGFEI YANG received the B.S. degree in information management and information system, and the M.S. degree in management science and engineering from the Dalian University of Technology, Dalian, Liaoning, in 2003 and 2005, respectively, and the Ph.D. degree in computer science and engineering from Waseda University, in 2009. He is currently a Professor with the Institute of Systems Engineering, Dalian University of Technology. His current research interests include business intelligence in big data environment and the Internet environment, data-driven management science, intelligent modeling, and sustainable development management.